Acupuncture and Herbal Medicine

# *Crocus sativus* L. produces anti-inflammatory effects and regulates the NLRP3–NF-κB pathway

Liang Yang[1], Huanhua Xu[2], Qian Hong[3], Nuo Xu[1], Yan Zhang[1], Rui Tao[1], Shuai Li[1], Zizheng Zhang[1], Jiahao Geng[1], Zihan Wang[1], Huizi Hu[1], Yan Dong[1], Zhaoyi Chu[1], Bin Zheng[1], Jinmiao Zhu[1], Ming Geng[1], Yue Gao[4,*]

*[1]School of Chemistry and Pharmaceutical Engineering, Hefei Normal University, Hefei, China; [2]National Key Laboratory for the Modernization of Classical and Famous Prescriptions of Chinese Medicine, Jiangxi University of Chinese Medicine, Nanchang, China; [3]Huaihai Hospital Affiliated to Xuzhou Medical University/PLA 71st Group Military Hospital, Xuzhou, China; [4]Beijing Institution of Radiation Medicine, Beijing, China*

**Abstract**

**Objective:** This study aimed to evaluate the anti-inflammatory effects of petal and stamen extracts of saffron crocus (*Crocus sativus*) and explore the underlying mechanism.

**Methods:** Local and systemic inflammation models were used to investigate the anti-inflammatory effects of *C. sativus.* A xylene-induced inflammation model or lipopolysaccharide (LPS)-induced inflammation model was used in this study. *C. sativus* petal and stamen extracts were each administered to the mice in the xylene and LPS models by gavage for 14 d at 0.1 and 0.4 g/kg doses, respectively. Enzyme-linked immunosorbent assay (ELISA) was used to measure the concentrations of tumor necrosis factor (TNF)-α and interleukin (IL)-1β in mouse serum. Hematoxylin and eosin (H&E) staining was used to observe the pathological changes in the ear in the xylene-induced inflammation model and in the spleen in the LPS-induced inflammation model. NOD-like receptor thermal protein domain associated protein 3 (NLRP3) protein levels within the nuclear factor-kappa B (NF-κB) pathway were assessed using western blotting. RAW264.7 cells were treated with LPS (5 μg/mL) and LPS + *C. sativus* (0.05, 0.1, and 0.2 mg/mL) for 24 h, and a Cell Counting Kit-8 was used to measure cell proliferation. Changes in NLRP3 and NF-κB levels were evaluated by western blotting.

**Results:** Petal and stamen extracts of *C. sativus* attenuated the anti-inflammatory effects in local or systemic inflammatory models and repaired pathological changes in the ear in the xylene-induced inflammation model and spleen in the LPS-induced inflammation model. These extracts also decreased the concentrations of TNF-α and IL-1β in the mouse serum in the LPS-induced inflammation model. *C. sativus* downregulated NLRP3 protein level through the NF-κB pathway and downregulated LC-3 and BECLIN1 *in vivo* and *in vitro*. Carbonyl Cyanide3-ChloroPhenylhydrazone (CCCP) weakened the effects of *C. sativus* on the NLRP3–NF-κB pathway.

**Conclusion:** *C. sativus* has anti-inflammatory effects and regulates the NLRP3-NF-κB pathway.

**Keywords:** Autophagy, *Crocus sativus* L., Inflammatory, NOD-like receptor thermal protein domain associated protein 3, Nuclear factor kappa B

**Graphical abstract:** http://links.lww.com/AHM/A86.

## Introduction

Saffron crocus (*Crocus sativus* L.) is a perennial herb belonging to the Iridaceae family and is extensively distributed in China, Greece, Egypt, Iran, Israel, Mexico, and Morocco[1]. The primary medicinal component of the plant consists of dried stigmas, which exhibit notable antiepileptic, anticonvulsant, antitumor, and sedative-hypnotic properties, as well as antihypertensive and antihyperlipidemic effects[2–4].

Stamens of C. *sativus* are used for medicinal purposes and exhibit anti-inflammatory, antioxidant, and skin-brightening properties. The key active phytoconstituents picrocrocin, crocin, crotecin, and safranal exhibit anti-inflammatory activity, exerting their effects primarily by modulating oxidative stress and regulating inflammatory factors such as tumor necrosis factor (TNF)-α, interleukin (IL)-1, and IL-10[5,6].

Autophagy is a cellular self-protective mechanism that is activated upon stimulation by the external environment. Autophagy plays a vital role in preserving cellular functions during the normal processes of cell metabolism and renewal. Autophagy imbalance is closely related to the development of many diseases, including tumors and inflammatory disorders[7]. Inflammation can enhance autophagy. It remains unclear whether this

*Liang Yang, Huanhua Xu, Qian Hong contributed equally to this work.*

**Corresponding author. Yue Gao, E-mail: gaoyue@bmi.ac.cn.*

*Received 16 June 2023 / Accepted 12 January 2024*

***How to cite this article:*** *Yang L, Xu HH, Hong Q, Xu N, Zhang Y, Tao R, Li S, Zhang ZZ, Geng JH, Wang ZH, Hu HZ, Dong Y, Chu ZY, Zheng B, Zhu JM, Geng M, Gao Y. Crocus sativus L. produces anti-inflammatory effects and regulates the NLRP3–NF-κB pathway. Acupunct Herb Med 2024;4(3):375–385. doi: 10.1097/HM9.0000000000000088*

enhancement serves as a mechanism for cellular self-repair, a pathological process culminating in cell death, or as a contributor to the occurrence and progression of diseases. Recent studies have shown that autophagy is involved in the initiation and progression of various diseases (including inflammation). Increasing evidence has shown that autophagy plays a vital role in the treatment of patients with tumors, myocardial infarction, and skin trauma[8].

The term "microinflammatory state" refers to the absence of apparent clinical signs of infection but the presence of mild and persistent inflammatory reactions. A microinflammatory state can elevate oxidative stress responses and activate NOD-like receptor thermal protein domain associated protein 3 (NLRP3) inflammasomes[9]. Inhibition of NLRP3 inflammasome expression significantly increases mitochondrial autophagy, slowing disease progression[10,11]. Various traditional Chinese medicines (TCMs) have been found to exert anti-inflammatory effects by enhancing mitochondrial autophagy and decreasing reactive oxygen species (ROS) production.

Inflammasomes are an important component of the innate immune system and protect against pathogenic microorganisms. There is a growing body of research on its involvement in autophagy[12]. Inflammatory cells specifically recognize intracytoplasmic pattern-recognition receptors, pathogen-associated molecular patterns, and endogenous injury-associated molecular patterns, leading to the activation of caspase-1 and subsequently facilitating the maturation and secretion of IL-1β, IL-18, and other inflammatory factors[13].

Four types of inflammasomes have been identified thus far: NLRP1, NLRP3, IPAF, and AIM2. Previous studies have primarily focused on the inflammasomes of the nucleotide-binding and oligomerization domain (NOD)-like receptor family (PYrin domain-containing 3, NLRP3), and there has been growing interest in determining the mechanism of action of the NLRP3 inflammasome[14]. NLRP3 activation can split the inactive pro-caspase-1 precursor to activate caspase-1. This activated caspase-1 cleaves pro-IL-1β and pro-IL-18 precursors, which become mature IL-1β and IL-18, leading to an aseptic inflammatory response and caspase-1–dependent cell death, namely, cell pyrosis[15].

Autophagy, on the other hand, is the response of eukaryotic cells to external stimuli. It is associated with the innate and adaptive immune systems and is closely associated with the NLRP3 inflammasome. Autophagy related protein 5 (ATG5) protein is a member of the autophagy-related gene family and plays an important regulatory role in the autophagy process. Studies have shown that the conserved ATG5-ATG12/ATG16 complex is essential for autophagosome formation, which is the result of triggering autophagy, a conserved process for the bulk degradation of cytoplasmic material through the creation of double membrane–bound vesicles called autophagosomes. The acetylation of ATG5 inhibits autophagosome maturation, whereas silent information regulator 3 (SIRT3), an important regulator of basal adenosine triphosphate (ATP) and overall energy homeostasis, can form a complex with ATG5 in cells to inhibit the acetylation of endogenous ATG5, thus promoting the maturation of autophagosomes. Nevertheless, the quantity of the NLRP3 inflammasome in SIRT3-deficient cells is significantly greater than that in normal cells[16], suggesting a potential regulatory relationship between autophagy and the NLRP3 inflammasome.

Many studies have shown that autophagy can negatively regulate the activation of NLRP3 inflammasome, thereby inhibiting the inflammatory response produced by the body and alleviating inflammatory tissue damage caused by diseases. The mechanism by which autophagy suppresses the NLRP3 inflammasome may involve a reduction in Asc Type Amino Acid Transporter (ASC) protein, NLRP3 protein phosphorylation, and the clearance of mitochondrial ROS. Autophagy has also been found to positively regulate NLRP3 inflammasome activation[17]. During starvation, autophagy can enhance the activation of caspase-1, promote the activation of inflammasomes, and increase the synthesis of pro-inflammatory cytokines, such as IL-1β and IL-18, through an ATG5-dependent non-classical pathway. Some cytoplasmic proteins lack signal peptides; thus, IL-1β, IL-18, and other pro-inflammatory factors cannot be degraded through the endoplasmic reticulum by autophagy. Instead, their excretion is promoted in the cytoplasm, which further aggravates inflammatory damage in tissues.

The occurrence and development of diseases are multifaceted. In numerous pathological scenarios, autophagy inhibits NLRP3 inflammasome activation, which prevents NLRP3 inflammasome-induced inflammation by reversing the autophagic effect. However, the specific mechanisms underlying this phenomenon remain unclear. Therefore, it is necessary to clarify whether *C. sativus* regulates the autophagy-mediated NLRP3–nuclear factor-kappa B (NF-κB) pathway. Therefore, it can be proven that a petal or stamen of *C. sativus* extract has anti-inflammatory effects.

## Materials and methods

### *Preparation of C. sativus extracts*

*C. sativus* L. was stored in a herbarium at the College of Life Sciences, Hefei Normal University (Herbarium No. ACE). The receptacles of *C. sativus* were removed and the petals were separated from the stamens. Petals were soaked in distilled water for 30 min and boiled for 1 h. The solution was filtered and collected. The filtrate was then centrifuged for 10 min to obtain the supernatant, which was diluted to 1 L using double-distilled water. The same procedure was repeated for *C. sativus* stamens to obtain an equivalent concentration of *C. sativus* stamen extract.

### *Ultra-performance liquid chromatography-mass spectrometry*

The key pharmacoactive components in the *C. sativus* powder were characterized using ultra-performance liquid chromatography (UPLC). Ultra-performance liquid chromatography-quadrupole time-of-flight mass spectrometry (UPLC/Q-TOF-MS) was performed (Synaptic G1, Waters, Milford, MA, USA) using a cooling autosampler and a column(ACQUITY UPLC HSS $T_3$ Column, 1.8 μm, 2.1 mm × 50 mm, 3/pk).

For chromatographic separation, an Acquity UPLC $T_3$ was used with a 1.8 μm (2.1 mm × 100 mm) chromatographic column operated at 45°C. The flow rate was 0.4 mL/min, and the indoor temperature was (20 ± 2)°C. The mobile phase consisted of phase A, an aqueous solution containing 0.1% formic acid (v/v), and phase B, an acetonitrile solution containing 0.1% formic acid (v/v). Column separation of *C. sativus* was performed using a gradient elution. Elution gradient: 0 to 1 min, 2.0% to 20% B; 1 to 27 min, 20% to 50% B; 29 to 30 min, 2% B.

The main parameters for mass spectrometry were set as follows: capillary voltage at 3.0 kV, taper hole voltage at 40 V, ion source temperature at 100°C, desolvent temperature at 350°C, gas flow rate of the taper hole at 450 L/h, desolvent gas flow rate at 900 L/h, and an injection volume of 5 μL. Leucine enkephalin was used to calibrate the mass spectrometry parameters with reference values of $[M + H]^+$ at 556.2771 and $[M-H]^-$ at 554.2615.

### Animals and groups

Healthy male Kunming (KM) mice (Beijing Vital River Laboratory Animal Technology Co., Ltd., Beijing, China), weighing (20 ± 2) g, were randomly divided into six groups. The mice were segregated and maintained at room temperature, with a photoperiod of 12 h and frequent air changes. The mice had access to food and water *ad libitum*. The research was conducted in accordance with the Animals (Scientific Procedures) Act 1986. The use of animals in this study was approved by the Animal Ethics Committee of Hefei Normal University (HFNUCM-2021013), and the design and implementation of the animal experiments complied with the 3R principle.

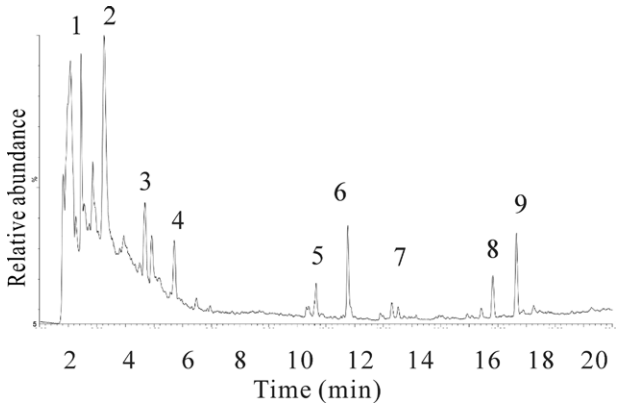


**Figure 1.** Ion flow diagram of *Crocus sativus* L. petal extraction detected using UPLC-Q/TOF-MS under the positive ion model. UPLC-Q/TOF-MS: Ultra-performance liquid chromatography-quadrupole time-of-flight mass spectrometry.

Two different animal models were used in the experiments.

(1) Xylene-induced inflammation model. First, 0.03 mL of xylene was evenly applied to the anterior and posterior surfaces of the right ear of mice, while the left ear was used as a control. After a 2 h period, the mice were weighed and humanely euthanized under ether anesthesia.

A rubber plug punch with a diameter of 7 mm was used to remove circular sections of the ears for weighing. The xylene-induced ear edema was quantified as the difference in weight between the xylene-treated right ear section and the untreated left ear section.

(2) Lipopolysaccharide (LPS)-induced inflammation model. Mice were treated with LPS (*Escherichia coli* 0111:B4; Sigma-Aldrich, Steinheim, Germany; 5 mg/kg body weight).

The *C. sativus* petal and stamen extracts were diluted with double-distilled water and administered daily by gavage for 14 d to the group of mice at doses of 0.1 and 0.4 g/kg, respectively, while the control group mice received double-distilled water of the same volume.

### Collection of tissues and plasma

On the 14th day, all the surviving animals were fasted overnight. Plasma was harvested through retro-orbital sinus blood collection, added to tubes with anticoagulant, and then centrifuged at 3,500×g for 10 min at 4°C. The mice were euthanized by cervical dislocation. The lungs, heart, spleen, kidneys, liver, and testes were collected. Portions of the tissue samples were stored in a –80°C freezer, and another portion was stored in formalin.

**Table 1**

**Identification of chemical constituents from *Crocus sativus* L. petal extract using UPLC-Q/TOF-MS in positive ion mode**

| Peak number | Name | Formulae | Neutral mass (m/z) | Experimental mass (m/z) | Error (ppm) |
|---|---|---|---|---|---|
| 1 | Trans-3-Gg | $C_{18}H_{54}O_{19}$ | 574.6214 | 574.5781 | 7.54 |
| 2 | Cis-4-GG | $C_{44}H_{64}O_{24}$ | 976.9790 | 976.9425 | 3.74 |
| 3 | Delphinidin-3,5-di-O-glucoside | $C_{27}H_{31}O_{17}$ | 627.5350 | 627.2612 | 4.34 |
| 4 | Myricetin-3-O-(2-O-glucosyl) glucoside | $C_{27}H_{30}O_{18}$ | 642.5271 | 642.6551 | 1.99 |
| 5 | Quercetin-di-O-glucoside | $C_{27}H_{30}O_{17}$ | 626.5271 | 626.5323 | 8.30 |
| 6 | Quercetin-di-O-glucoside·$H_2O$ | $C_{27}H_{30}O_{17}.H_2O$ | 644.5430 | 644.6304 | 1.36 |
| 7 | Kaempferol | $C_{15}H_{10}O_6$ | 286.2399 | 286.2234 | 5.80 |
| 8 | Petunidin-3,5-di-O-glucoside | $C_{28}H_{33}O_{17}$ | 641.5616 | 641.5186 | 6.70 |
| 9 | Kaempferol-tri-O-glucoside (with an acetyl moiety) | $C_{35}H_{42}O_{22}$ | 814.7080 | 814.7420 | –4.20 |

UPLC-Q/TOF-MS: Ultra-performance liquid chromatography-quadrupole time-of-flight mass spectrometry.

### *Hematoxylin and eosin staining*

Ear tissue from the xylene-induced inflammation model and spleen tissue from the LPS-induced inflammation model were fixed in 10% formalin, dehydrated in ethanol, and embedded in paraffin. Ear and spleen paraffin blocks were cut into 4 μm sections, which were subjected to hematoxylin and eosin (H&E) staining and then viewed by light microscopy. Sections from each animal were selected and 10 random microscopic fields at 400× magnification were captured from each slide to observe histopathological changes. H&E staining was performed using an optical microscope. Ear and spleen tissue sections from three animals were selected from each group.

### *Western blot analysis*

Proteins were extracted from frozen ear and spleen tissues using radioimmunoprecipitation assay (RIPA) lysis buffer, and protein concentrations were measured using a Bicinchoninic Acid Assay (BCA) protein assay kit (Beyotime, Shanghai, China). Protein samples were separated by 10% sodium dodecyl sulfate (SDS) polyacrylamide gel electrophoresis and transferred to polyvinylidene difluoride (PVDF) membranes (Millipore, Bedford, MA, USA). The membranes were blocked in 5% non-fat powdered milk or bovine serum albumin (BSA) at room temperature for 1 h and then incubated with primary antibodies at 4°C overnight. The following primary antibodies were used: IL-1β (1:1,000; ab254360, Abcam, Cambridge, England), TNF-α (1:1,000; ab215188, Abcam), BECLIN1 (1:1,000; 3459s, CST), LC-3 (1:1,000; ab48394, Abcam), and GAPDH (1:3,000, Abcam). After three washes in Tris-buffered saline (TBS) containing 0.1% Tween-20 (TBST), the membranes were incubated with anti-rabbit IgG secondary antibody conjugated to horseradish peroxidase (HRP) for 1 h (1:5,000, ab6721, Abcam). Finally, the protein bands were visualized by enhanced chemiluminescence (ECL) reagent using the Tanon 6100 automatic chemiluminescence image analysis system (Tanon Science & Technology Co., Shanghai, China) and analyzed using ImageJ software (National Institutes of Health, Bethesda, MD, USA).

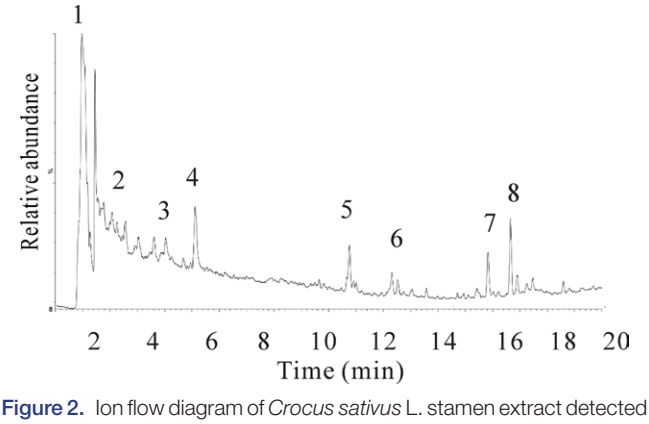


**Figure 2.** Ion flow diagram of *Crocus sativus* L. stamen extract detected using UPLC-Q/TOF-MS under the positive ion model. UPLC-Q/TOF-MS: Ultra-performance liquid chromatography-quadrupole time-of-flight mass spectrometry.

### *Enzyme-linked immunosorbent assay*

Enzyme-linked immunosorbent assay (ELISA) was used to measure the concentrations of TNF-α and IL-1β in mouse serum, according to the manufacturer's instructions (Wuhan Service Biotechnology Co., Ltd., Wuhan, China).

### *Cell culture and groups*

Murine macrophage RAW264.7, acquired from the Cell Bank of the Chinese Academy of Sciences, was cultured in Dulbecco modified Eagle's medium (DMEM; Servicebio, Wuhan, China) supplemented with 10% fetal bovine serum (FBS; Gibco, Grand Island, NY, USA) and antibiotics (Beyotime Biotechnology, Shanghai, China) in a conventional incubator with 5% carbon dioxide at 37°C.

Cells were treated with LPS (5 μg/mL), LPS + *C. sativus* L. (0.05 mg/mL), LPS + *C. sativus* L. (0.1 mg/mL), or LPS + *C. sativus* L. (0.2 mg/mL) for 24 h. RIPA lysis buffer (Servicebio) with phosphatase inhibitor (Servicebio) and protease inhibitor cocktail (Servicebio) was used to lyse the cultured cells. The protein levels were measured using a BCA Protein Assay Kit (Beyotime Biotechnology).

**Table 2**

**Identification of chemical constituents of *Crocus sativus* L. stamen extract by UPLC-Q/TOF-MS in the positive ion mode**

| Peak number | Name | Formulae | Neutral mass (m/z) | Experimental mass (m/z) | Error (ppm) |
|---|---|---|---|---|---|
| 1 | Crocetin | $C_{20}H_{24}O_4$ | 328.4046 | 328.4841 | –2.40 |
| 2 | Trans-3-Gg | $C_{18}H_{54}O_{19}$ | 574.6214 | 574.5781 | 7.54 |
| 3 | Cis-4-GG | $C_{44}H_{64}O_{24}$ | 976.9790 | 976.9425 | 3.74 |
| 4 | Rutin | $C_{27}H_{30}O_{16}$ | 610.6271 | 610.6758 | –0.80 |
| 5 | 2,4,4-trimethyl-3-formyl-6-hydroxy-2,5-cyclohexadien-1-one | $C_{10}H_{14}O_3$ | 182.2182 | 182.2704 | –2.90 |
| 6 | Quercetin-di-O-glucoside·$H_2O$ | $C_{27}H_{30}O_{17}.H_2O$ | 644.5430 | 644.6304 | 1.36 |
| 7 | Petunidin-3,5-di-O-glucoside | $C_{28}H_{33}O_{17}$ | 641.5616 | 641.5186 | 6.70 |
| 8 | Kaempferol-tri-O-glucoside (with an acetyl moiety) | $C_{35}H_{42}O_{22}$ | 814.7080 | 814.7420 | –4.20 |

UPLC-Q/TOF-MS: Ultra-performance liquid chromatography-quadrupole time-of-flight mass spectrometry.

### *Autophagy staining assay kit with monodansylcadaverin*

The cells were treated with LPS (5 μg/mL), LPS + *C. sativus* L. (0.2 mg/mL), LPS + CCCP (5 μmol/L), and LPS + *C. sativus* L. + CCCP for 24 h. The cells were harvested in centrifuge tubes and suspended in phosphate-buffered saline (PBS) containing Triton X-100. Monodansylcadaverin (MDC) was added and the mixture was gently mixed in the dark for 30 min. The cells were resuspended and covered with glass slides before being observed and photographed using a fluorescence microscope.

### *Statistical analysis*

SAS statistical software (SAS Institute Inc., Cary, NC, USA) was used to determine differences between the groups. All data are presented as mean ± standard deviation (SD), and statistical significance was set at $P < 0.05$. The figures were processed and displayed using GraphPad Prism software (version 5.01; GraphPad Software, San Diego, CA, USA), and the images were processed using the CorelDRAW Graphics Suite 2019 (Corel Corporation, Ottawa, ON, Canada). Results with a $P$ value <0.05 were considered statistically significant.

## Results

### *Identification and characterization of the chemical compounds in C. sativus*

To identify significant and potentially active phytoconstituents, *C. sativus* petal and stamen extracts were analyzed using high-performance liquid chromatography-mass spectrometry. Chromatograms of the *C. sativus* petal extract in positive ionization mode are shown in Figure 1. These compounds were identified as potential active ingredients in *C. sativus* petals; detailed information regarding these compounds is presented in Table 1. Chromatograms of *C. sativus* stamen extracts in the positive ion mode are depicted in Figure 2. The compounds

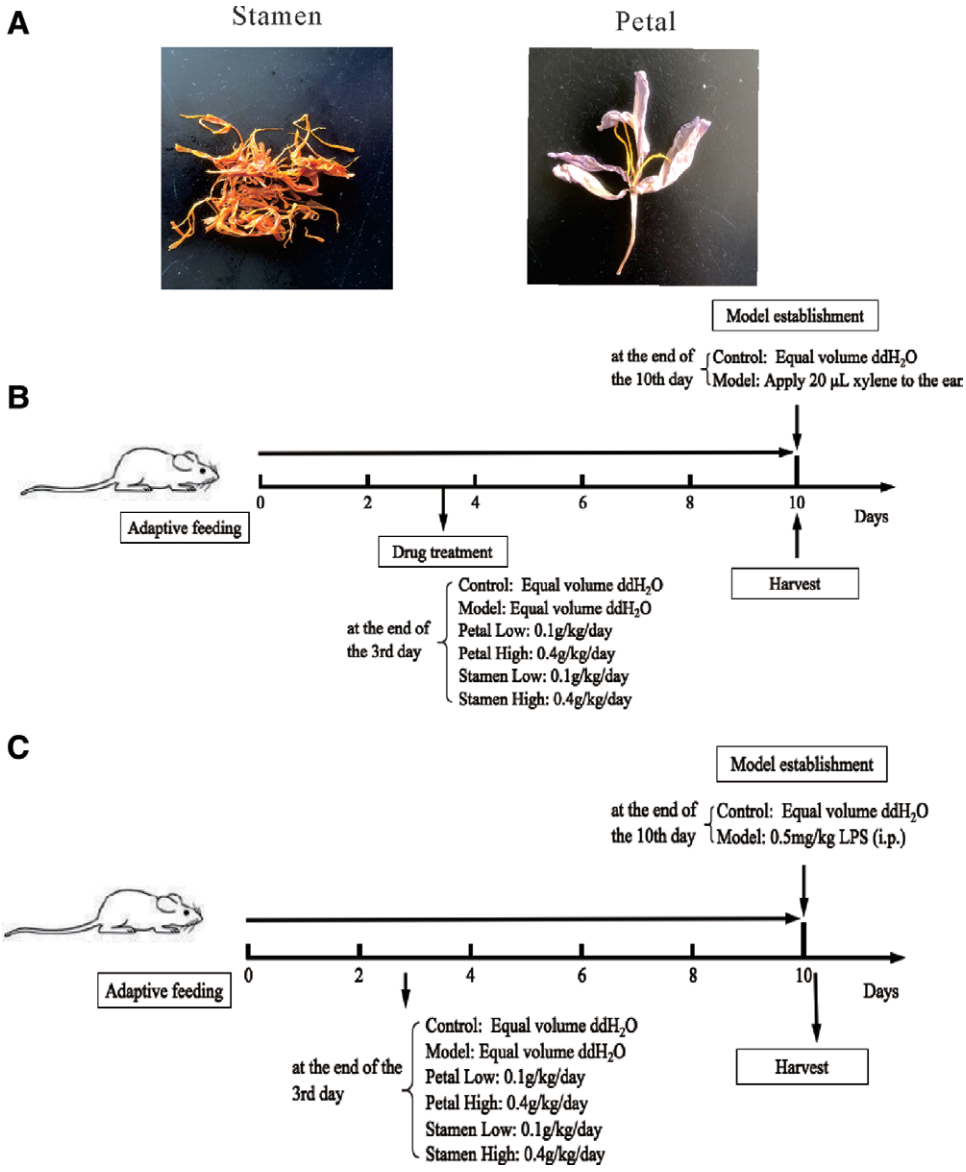


**Figure 3.** The experimental design for evaluating the therapeutic effect of *Crocus sativus* L. on local and systematic inflammation models induced by xylene or LPS. (A) The specimen shape of stamen and petal; (B) The experimental design for evaluating the local inflammatory effect of *C. sativus* L. on mice induced by xylene; (C) The experiment design for evaluating the systematic inflammatory effect of *C. sativus* L. on mice induced by LPS. $ddH_2O$: Double distilled water; LPS: Lipopolysaccharide.

identified as potential active ingredients in *C. sativus* stamens are presented in Table 2, along with detailed information. The experimental design of the therapeutic effects of *C. sativus* L. is shown in Figure 3.

The compounds were identified as potential active ingredients in *C. sativus* L. petals, and detailed information regarding these compounds is presented in Table 1.

### *C. sativus attenuated the local inflammatory effect induced by xylene*

Xylene-induced ear edema in mice was represented by the difference in weight between the model and control groups. As shown in Figure 4, the mean ear index in the model group was significantly higher than that in the control group. *C. sativus* petal and stamen extracts attenuated the weight increase caused by xylene-induced ear inflammation.

The average ear index was lower in the low-dose *C. sativus* petal group than in the model group. Similarly, the average ear index was lower in the high-dose *C. sativus* group than that in the model group. The average ear index in the low-dose *C. sativus* stamen group was lower than that in the model group, and that in the high-dose group was lower than that in the model group.

### *C. sativus attenuated the systematic inflammatory effects induced by LPS*

*C. sativus* treatment attenuated LPS-induced inflammatory effects. As shown in Figure 5, diarrhea, messy fur, poor mental state, and splenic swelling were evident in the mice that received LPS. LPS-induced splenic edema was evident from the average spleen index of the model group, which was significantly higher than that of the control group. The therapeutic effects of *C. sativus* petal and stamen extracts were reflected in the average spleen indices of the petal low (PL), petal high (PH), stamen low (SL), and stamen high (SH) groups, which were significantly lower than those of the model group. H&E staining was performed to evaluate the effects of *C. sativus* on LPS-induced inflammation

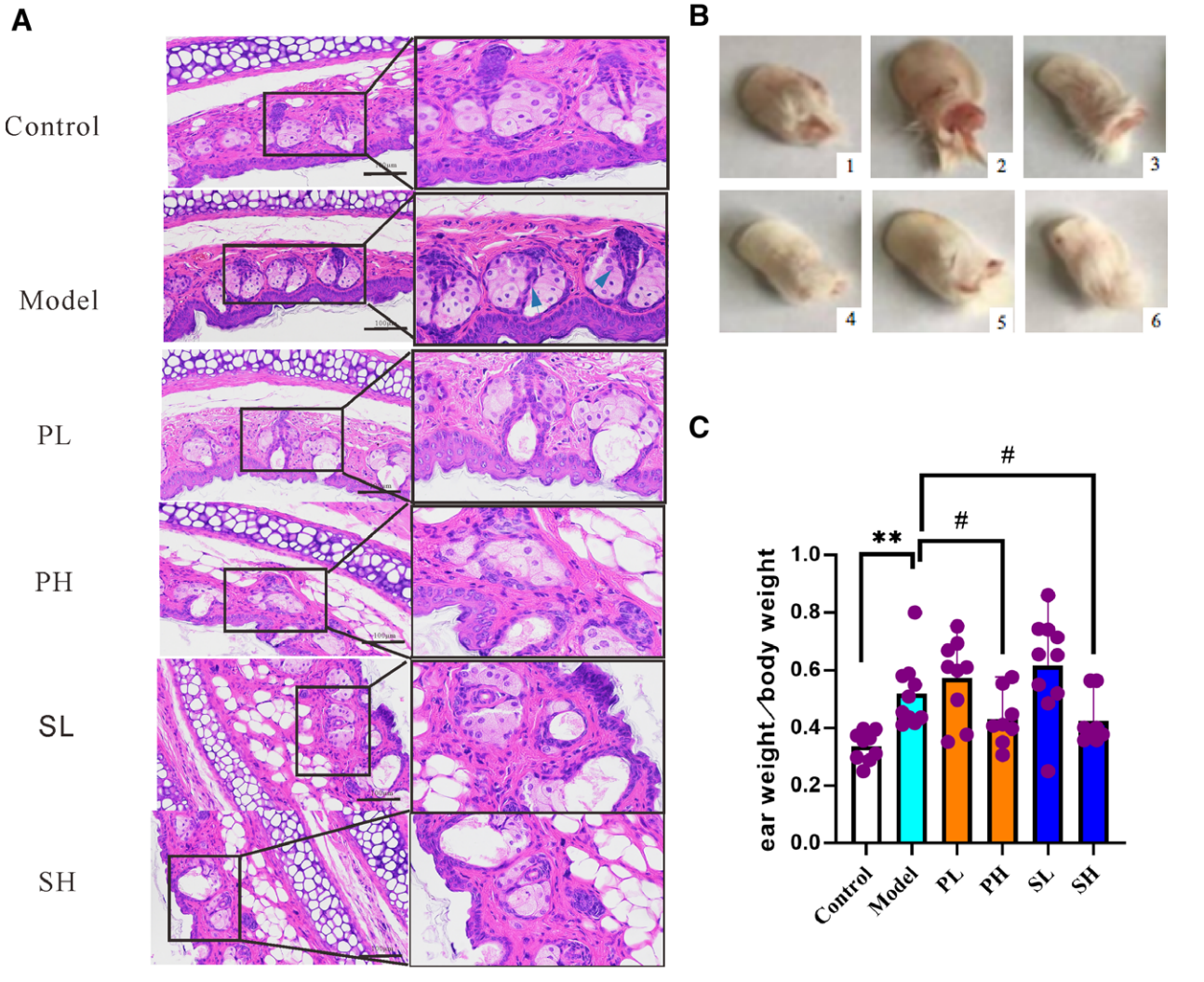


**Figure 4.** The therapeutic effect of *Crocus sativus* L. on local inflammation induced by xylene. (A) Representative histological sections of ear cross-sections (H&E staining, as shown by the green arrow). (B) Representative photographs of mouse ears. (1) Control group; (2) model group; (3) model + PL group; (4) model + PH; (5) model + SL; (6) model + SH; and (C) effects of *C. sativus* L. on the organ coefficient (EW/BW) in mice (mean ± SD, $n = 8–10$). $^{**}P < 0.01$ *versus* control; $^{\#}P < 0.05$ *versus* model. Groups: control, model (0.03 mL xylene), PL (model + petal 0.1 g/kg), PH (model + petal 0.4 g/kg), SL (model + stamen 0.1 g/kg), SH (model + stamen 0.4 g/kg). BW: Body weight; EW: Ear weight; H&E: Hematoxylin and eosin; PH: Petal high; PL: Petal low; SD: Standard deviation; SH: Stamen high; SL: Stamen low.

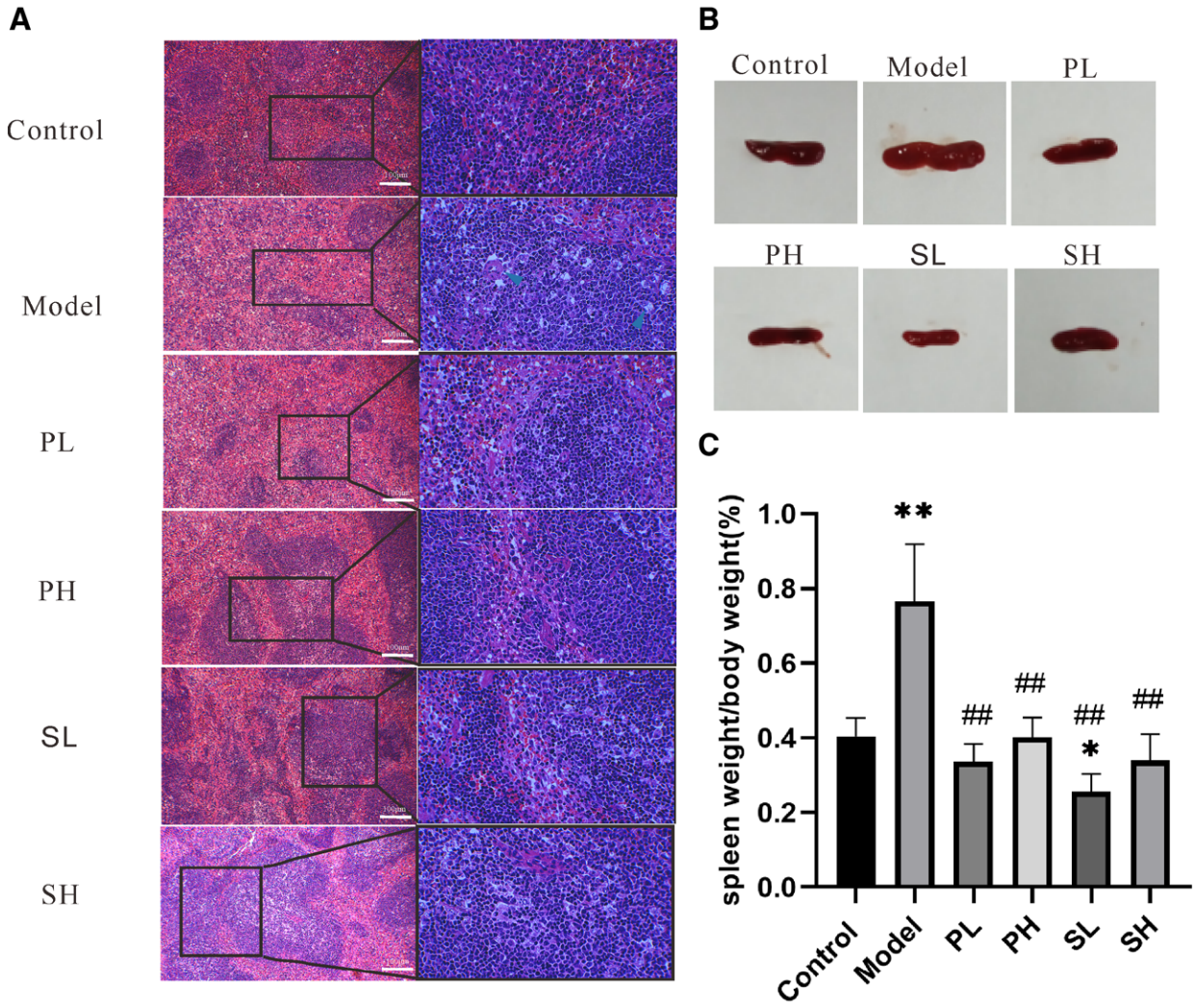


**Figure 5.** The therapeutic effect of *Crocus sativus* L. in a systematic inflammation model induced by LPS. (A) Representative histological sections of cardiomyocyte cross-sections (H&E staining, as shown by the blue arrow). (B) Representative images of mouse spleen. (C) Effects of *C. sativus* L. on the organ coefficient (SW/BW) in mice (mean ± SD, $n = 8–10$). *$P < 0.05$, **$P < 0.01$ *versus* control; $^{\#\#}P < 0.01$ *versus* model. Groups: control, model (LPS 5 mg/kg), PL (model + petal 0.1 g/kg), PH (model + petal 0.4 g/kg), SL (model + stamen 0.1 g/kg), SH (model + stamen 0.4 g/kg). BW: Body weight; H&E: Hematoxylin and eosin; LPS: Lipopolysaccharide; PH: Petal high; PL: Petal low; SD: Standard deviation; SH: Stamen high; SL: Stamen low;.

in mice. Compared with the control group, inflammatory infiltration increased in the model group, and tissue edema was evident in the spleens of mice.

### *C. sativus regulates the NLRP3 pathway and attenuates the systematic effect*

The petal and stamen extracts of *C. sativus* decreased the concentrations of TNF-α and IL-1β in mouse serum in the LPS-induced inflammation model (Figure 6). *C. sativus* downregulated the levels of NLRP3 protein through the NF-κB pathway and the autophagy-related proteins LC-3 and BECLIN1 in a mouse model of LPS-induced inflammation. However, the level of the LAMP1 protein was downregulated, and *C. sativus* attenuated this change. Therefore, we examined the effect of *C. sativus* on LPS-induced inflammation in RAW264.7 cells.

*C. sativus* reduces the effects of LPS on the proliferation of RAW264.7 cells (Figure 7). *C. sativus* also downregulated the levels of the NLRP3 NF-κB and BECLIN1 proteins in LPS-induced inflammation in RAW264.7 cells. In an LPS-induced inflammation model, LAMP1 was also downregulated in RAW264.7, and *C. sativus* attenuated this change (Figure 8). After the addition of carbonyl cyanide 3-chlorophenylhydrazone, the effect of *C. sativus* on the NLRP3–NF-κB pathway weakened.

## Discussion

The onset and progression of inflammation are frequently associated with a plethora of illnesses, including cardiovascular diseases and malignancies. There is abundant data regarding the application of TCM to treat inflammation[18]. Studies of various anti-inflammatory TCMs have indicated that *C. sativus* is frequently used to treat inflammation. Additionally, *C. sativus* has the characteristics of low toxicity and wide range, which already was brought into 2020 management "according to tradition since food is the material directory of Chinese medicinal materials". Therefore, it is essential to elucidate the anti-inflammatory mechanisms of *C. sativus*. This understanding is crucial for enhancing the

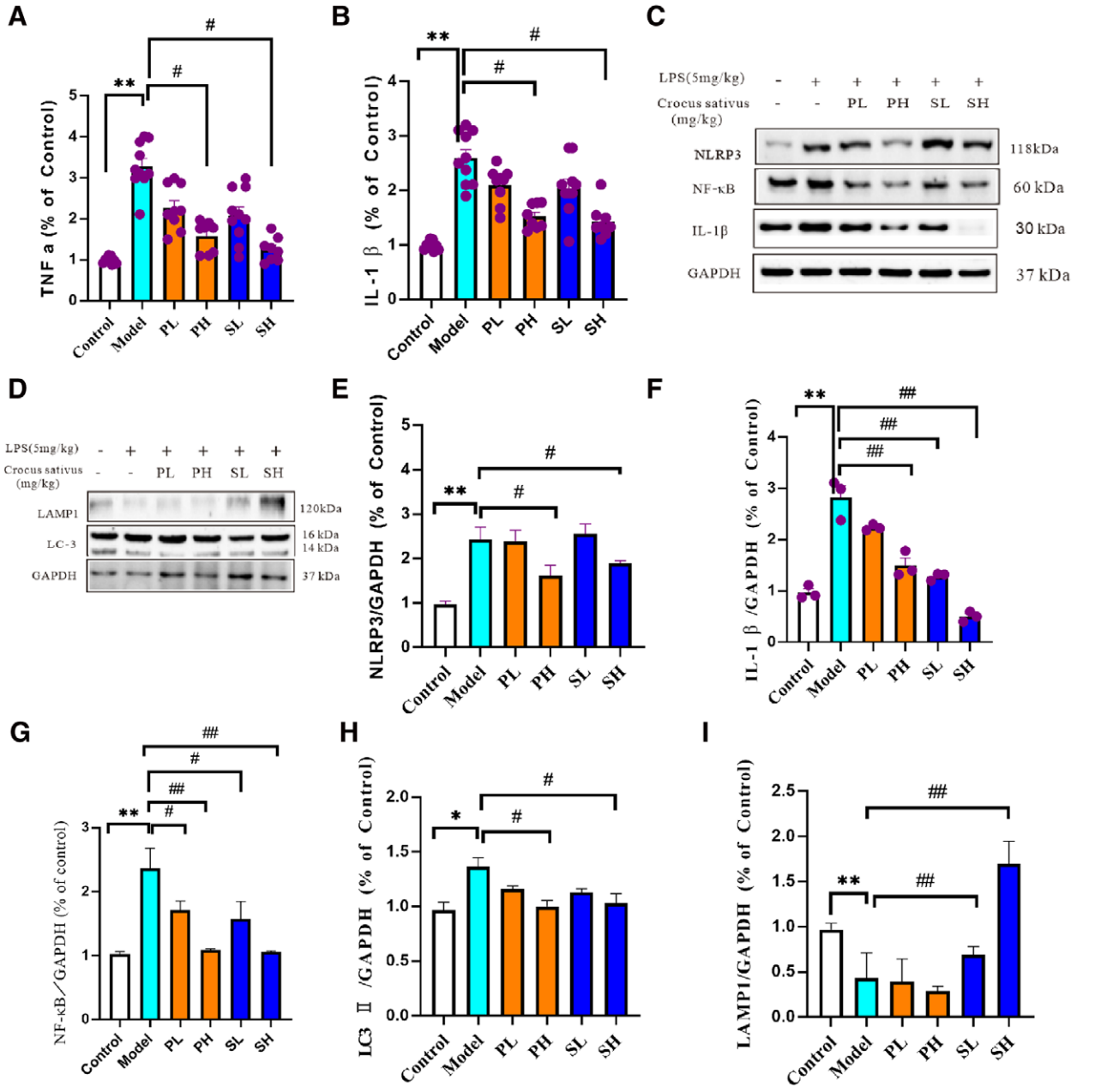


**Figure 6.** Effects of *Crocus sativus* L. on the NLRP3 pathway and autophagy-related protein expression in LPS-induced systemic inflammatory model mice. (A–B) Representative concentrations of IL-1β and TNF-α in serum, respectively. (C–D) Representative western blots for NLRP3, IL-1β, NF-κB, LC-3, and LAMP1 proteins. (E–I) Corresponding quantitative analyses of NLRP3, IL-1β, NF-κB, LC-3, and LAMP1. Data are expressed as the mean ± SD, $n = 6$ for ELISA and $n = 3$ for western blotting. $^{*}P < 0.05$, $^{**}P < 0.01$ *versus* control; $^{\#}P < 0.05$, $^{\#\#}P < 0.01$ *versus* model (Student *t* test). ELISA: Enzyme-linked immunosorbent assay; GAPDH: Glyceraldehyde-3-phosphate dehydrogenase; IL-1β: Interleukin-1β; LPS: Lipopolysaccharide; NF-κB: nuclear factor-kappa B; NLRP3: NOD-like receptor thermal protein domain associated protein 3; PH: Petal high; PL: Petal low; SD: Standard deviation; SH: Stamen high; SL: Stamen low; TNF: Tumor necrosis factor.

prognosis, optimizing the utilization of *C. sativus*, and determining precise dosage levels to achieve the most effective anti-inflammatory outcomes.

*C. sativus* belongs to the iris family and is commonly referred to as saffron crocus, owing to the saffron color of the dried stigmas of its flowers[3,4]. Most of the saffron in the worldwide spice trade is grown in Iran, Afghanistan, India, and Spain. Studies have shown that the main components of saffron are crocusic acid, crocusin, amygdalin, and crocusal acid. In recent years, various animal studies have shown that saffron has antitumor, anti-depressive, anti-anxiety, anti-Alzheimer, anti-inflammatory, hypnotic, and anti-diabetic properties.

Picrocrocin, crocin, crotecin, and safranal are anti-inflammatory agents found in *C. sativus*[5]. They play an anti-inflammatory role by influencing oxidative stress and regulating inflammatory factors, such as TNF-α, IL-1, and IL-10. The 2020 edition of the Pharmacopoeia of the People's Republic of China mentions a limited list of the main components of *C. sativus* but does not specify the components and amounts found in extracts from the different plant parts. This omission stems from existing scientific uncertainties, such as determining the active component responsible for its anti-inflammatory action, identifying its target, and understanding the pathways through which it exerts its anti-inflammatory effects.

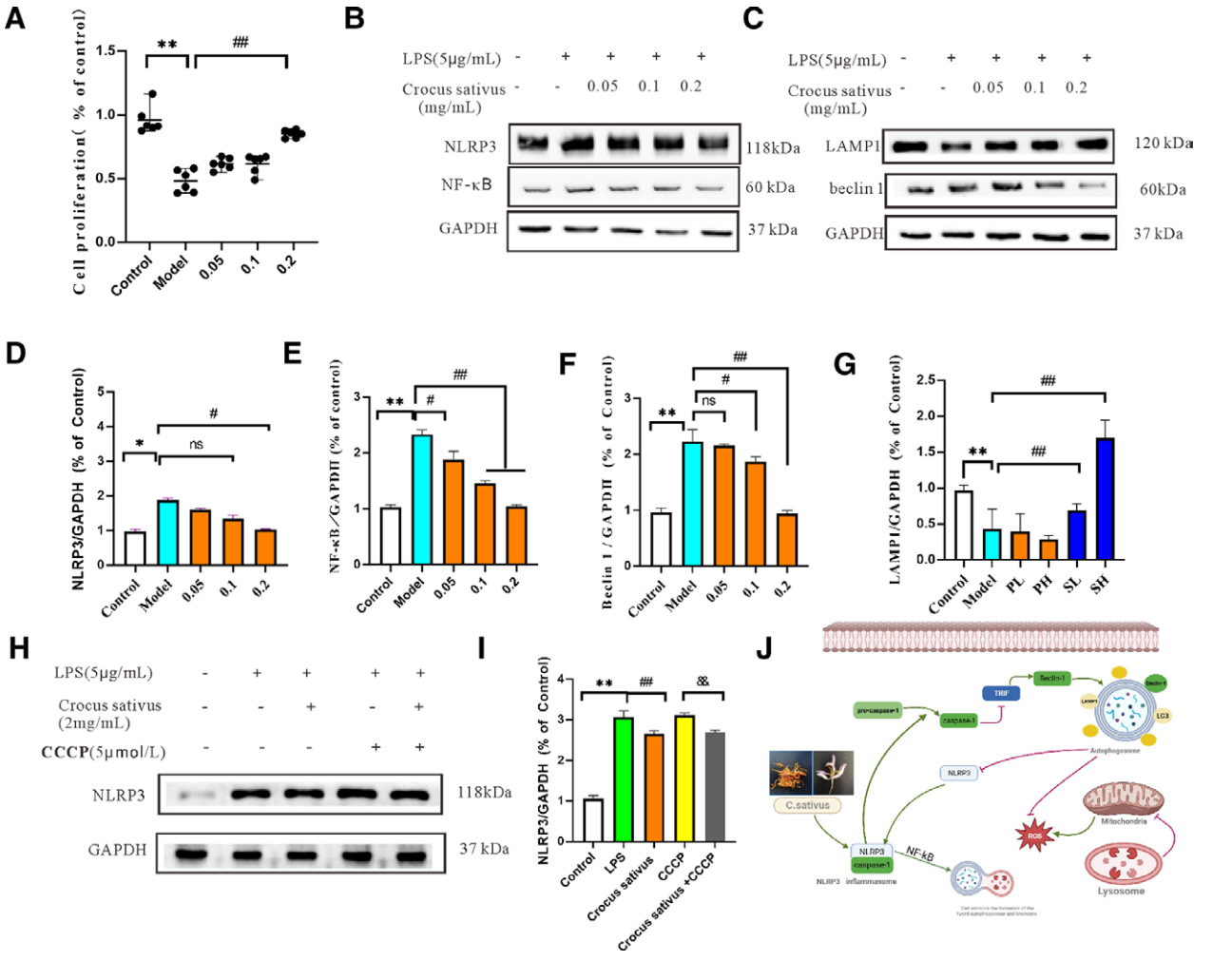


**Figure 7.** Effects of *Crocus sativus* L. (stamen) on NLRP3 pathway and autophagy-related protein expression in RAW264.7 cell inflammatory model induced by LPS (5 μg/mL). (A) Representative cell proliferation assay using the CCK8 method (24 h). (B–C) Representative western blots for NLRP3, NF-κB, BECLIN1, and LAMP1 proteins. (D–G) Corresponding quantitative analyses of NLRP3, NF-κB, BECLIN1, and LAMP1. (H) Representative western blot of NLRP3 expression. (I) Corresponding quantitative analyses of NLRP3; data are expressed as mean ± SD, $n = 6$ for CCK8, and $n = 3$ for western blotting. $^{*}P < 0.05$, $^{**}P < 0.01$ *versus* control; $^{\#}P < 0.05$, $^{\#\#}P < 0.01$; *versus* model; $^{\&\&}P < 0.01$ *versus C. sativus* group (Student *t* test). (J) The anti-inflammatory effects of *C. sativus* and the relationship between the NLRP3 inflammasome and autophagy during the inflammatory phase. GAPDH: Glyceraldehyde-3-phosphate dehydrogenase; LPS: Lipopolysaccharide; NF-κB: nuclear factor-kappa B; NLRP3: NOD-like receptor thermal protein domain associated protein 3; SD: Standard deviation.

Girme et al.[14] constructed a fingerprint of Kashmiri saffron and found that different extracts (stigmas, stamens, and petals) contained oleanderous compounds (matrine, crocin, crocin ester, and crosaffron aldehyde), terpenoids, and flavonoids (glycoconjugates of kamanol), indicating that different extracts from various parts of *C. sativus* may have different effects[19]. According to our UPLC-MS results, the components of stamens and petals were different. We observed that petal and stamen extracts of *C. sativus* attenuated inflammation in local or systemic inflammatory models, repaired pathological changes in the ear in a xylene-induced inflammation model or spleen in an LPS-induced inflammation model, and decreased the concentrations of TNF-α and IL-1β in mouse serum in an LPS-induced inflammation model.

Autophagy is a response of eukaryotic cells to external stimuli and is associated with the innate and adaptive immune systems[20]. Autophagy enhances NLRP3 phosphorylation, leading to ROS clearance. Activation of the NLRP3 inflammasome promotes the transformation of inactive pro-caspase-1 into its active form, caspase-1. Following this activation, caspase-1 cleaves TRIF, leading to a decrease in the induction of BECLIN1 by TRIF. Consequently, autophagy is inhibited by reduced levels of BECLIN1. Simultaneously, the administration of *C. sativus* reduced autophagic vacuoles (autophagosomes) and enhanced the formation of autophagosome-lysosome fusion through the NLRP3-NF-κB pathway, which is also closely related to the NLRP3 inflammasome. Research findings indicate that the acetylation of ATG5 hinders the maturation of autophagosomes, whereas SIRT3 has the capacity to form a complex with ATG5 within cells, preventing the acetylation of endogenous ATG5 and consequently facilitating the maturation of autophagosomes. In our study, the number of NLRP3 inflammasomes in SIRT3-deficient cells was much higher than that in normal cells. Therefore, it can be speculated that there is a regulatory relationship between autophagy and NLRP3 inflammasome[15].

Numerous studies have shown that autophagy can negatively regulate the activation of NLRP3 inflammasome, thereby inhibiting the inflammatory response

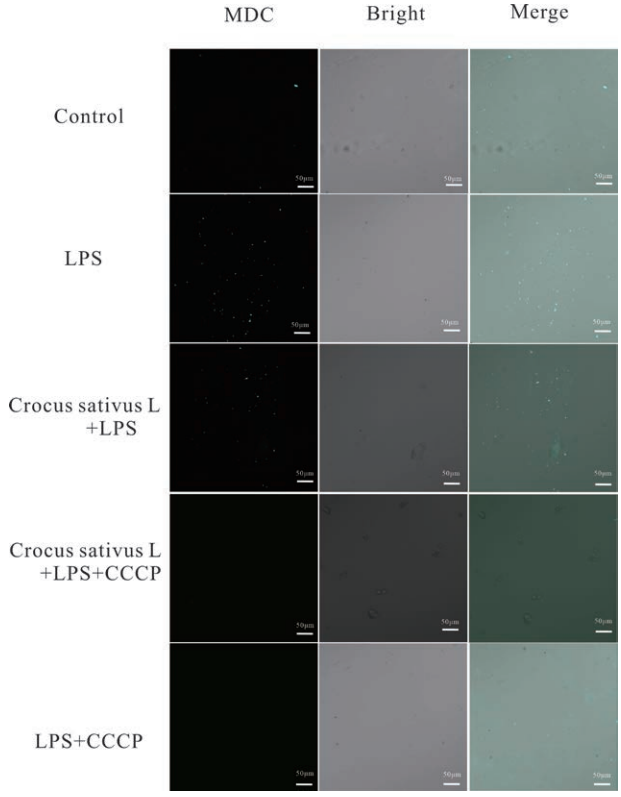


**Figure 8.** Effects of *Crocus sativus* L. (stamen) on autophagy in RAW264.7 cell inflammatory model induced by LPS (5 μg/mL) (MDC staining). CCCP: Carbonyl Cyanide3-ChloroPhenylhydrazone; LPS: Lipopolysaccharide; MDC: monodansylcadaverin.

produced by the body and alleviating inflammatory damage to tissues caused by diseases[16]. The mechanism by which autophagy suppresses the NLRP3 inflammasome could be associated with several factors, including a reduction in ASC protein levels, phosphorylation of the NLRP3 protein, and the removal of mitochondrial ROS. Autophagy positively regulates NLRP3 inflammasome activation by regulating USP22, which inhibits NLRP3 inflammasome activation by promoting ATG5-mediated macroautophagy/autophagy[16].

Autophagy under starvation can enhance the activation of caspase-1, promote the activation of inflammasomes, and increase the synthesis of pro-inflammatory cytokines such as IL-1β and IL-18 through an ATG5-dependent non-classical pathway. Some cytoplasmic proteins that lack signaling peptides, such as IL-1β, IL-18, and other pro-inflammatory factors, cannot be degraded through the endoplasmic reticulum and enter autophagy but promote their excretion in the cytoplasm, further aggravating the inflammatory damage of tissues[15]. *C. sativus* downregulated the levels of NLRP3 protein through the NF-κB pathway and autophagy-related proteins *in vivo* and *in vitro*. After adding carbonyl cyanide 3-chlorophenylhydrazone, the effect of *C. sativus* on the NLRP3–NF-κB pathway weakened. This indicates that the effect of *C. sativus* on the NLRP3–NF-κB pathway may occur *via* autophagy.

Autophagy is a self-protective process that occurs in cells after external stimulation and is necessary for normal cell metabolism and renewal. Autophagy involves phagophores, autophagosomes, and autolysosomes[9,13]. During autophagy, the membrane structures of the endoplasmic reticulum and mitochondria in the cytoplasm of cells form a precursor of autophagy with a double-membrane cup. The septum continuously extends and gradually wraps around cell waste to form closed autophagosome vesicles. Finally, the autophagosome and lysosome fuse to form an autophagolysosome, which degrades encapsulated cellular components and recycles the degradation products. Autophagosomes need to fuse with lysosomes, a process facilitated by the endosomal maturation complex and the monomeric GTP enzyme (RabS), in order to transform into autophagolysosomes through microtubule-based retransport.

Lysosome-related proteins include LAMP1, LAMP2, and UVRAG. When the lysosomal membrane is compromised, resulting in a decrease in lysosomal hydrolase activity, amino acids, and proteins generated during the degradation process serve as essential resources for cells, providing nutrients, energy, or recycling. *C. sativus* downregulated the autophagy-related proteins LC-3 and BECLIN1 but upregulated the expression of LAMP1. These findings suggest that *C. sativus* may reduce autophagy bubbles (autophagosomes) and enhance the formation of fused autophagosomes and lysosomes, thereby decreasing the damage caused by autophagosomes, which is related to the NLRP3–NF-κB pathway.

## Conclusion

Petal and stamen extracts of Petal and stamen extracts of *C. sativus* attenuated the anti-inflammatory effects in local or systemic inflammatory models. *C. sativus* repaired pathological changes in the ear in the xylene-induced inflammation model and spleen in the LPS-induced inflammation model. *C. sativus* plays an anti-inflammatory role by regulating autophagy and the NLRP3–NF-κB pathway.

## Conflict of interest statement

Yue Gao is an editorial board member of the journal. None of the other authors declare any conflicts of interest.

## Funding

This work was supported by the National Natural Science Foundation of China (81873063); High-level talents Research project of Hefei Normal University (2020rcjj30); Key Project of Provincial Scientific Research Platform of Hefei Normal University in 2020 (2020PTZD14); Key Project of Universities Natural Science Foundation of Anhui province (KJ2021A0935, KJ2021A0932). Innovation Team and Talents Cultivation Program of National Administration of Traditional Chinese Medicine (ZYYCXTD-C-202009).

## Author contributions

Data curation: Zihan Wang and Yan Zhang; Funding acquisition: Liang Yang and Yue Gao; Investigation: Liang Yang, Qian Hong, and Huizi Hu; Resources: Yan Dong; Software: Huan Hua Xu; Supervision: Yue Gao;

Visualization: Nuo Xu, Rui Tao, and Ming Geng; Writing – original draft: Liang Yang and Bin Zheng; Writing – review & editing: Jinmiao Zhu. All authors have read and agreed to the published version of the manuscript.

## Ethical approval of studies and informed consent

The use of animals in this study was approved by the Animal Ethics Committee of Hefei Normal University (HFNUCM-2021013).

## Acknowledgments

We thank the support from "Anhui Engineering Laboratory for Medicinal and Food Homologous Natural Resources Exploration."

## Data availability

All data generated or analyzed during this study are included in this published article.

## References

[1] Khorasanchi Z, Shafiee M, Kermanshahi F, et al. Crocus sativus a natural food coloring and flavoring has potent anti-tumor properties. *Phytomedicine* 2018;43:21–27.
[2] Bukhari SI, Manzoor M, Dhar MK. A comprehensive review of the pharmacological potential of Crocus sativus and its bioactive apocarotenoids. *Biomed Pharmacother* 2018;98:733–745.
[3] Li K, Li Y, Ma Z, et al. Crocin exerts anti-inflammatory and anti-catabolic effects on rat intervertebral discs by suppressing the activation of JNK. *Int J Mol Med* 2015;36(5):1291–1299.
[4] Hatziagapiou K, Lambrou GI. The protective role of Crocus Sativus L. (Saffron) against ischemia-reperfusion injury, hyperlipidemia and atherosclerosis: nature opposing cardiovascular diseases. *Curr Cardiol Rev* 2018;14(4):272–289.
[5] Poillet-Perez L, White E. Role of tumor and host autophagy in cancer metabolism. *Genes Dev* 2019;33(11–12):610–619.
[6] Matsuzawa-Ishimoto Y, Hwang S, Cadwell K. Autophagy and inflammation. *Annu Rev Immunol* 2018;36:73–101.
[7] Mowers EE, Sharifi MN, Macleod KF. Functions of autophagy in the tumor microenvironment and cancer metastasis. *FEBS J* 2018;285(10):1751–1766.
[8] Deretic V. Autophagy in inflammation, infection, and immunometabolism. *Immunity* 2021;54(3):437–453.
[9] Yang H, Lv H, Li H, et al. Oridonin protects LPS-induced acute lung injury by modulating Nrf2-mediated oxidative stress and Nrf2-independent NLRP3 and NF-κB pathways. *Cell Commun Signal* 2019;17(1):62.
[10] Xiong Y, Chen L, Fan L, et al. Free total rhubarb anthraquinones protect intestinal injury *via* regulation of the intestinal immune response in a rat model of severe acute pancreatitis. *Front Pharmacol* 2018;9:75.
[11] Wang L, Hauenstein AV. The NLRP3 inflammasome: mechanism of action, role in disease and therapies. *Mol Aspects Med* 2020;76:100889.
[12] Liu P, Huang G, Wei T, et al. Sirtuin 3-induced macrophage autophagy in regulating NLRP3 inflammasome activation. *Biochim Biophys Acta Mol Basis Dis* 2018;1864(3):764–777.
[13] Houtman J, Freitag K, Gimber N, et al. Beclin1-driven autophagy modulates the inflammatory response of microglia *via* NLRP3. *EMBO J* 2019;38(4):e99430.
[14] Girme A, Pawar S, Ghule C, et al. Bioanalytical method development and validation study of neuroprotective extract of Kashmiri saffron using ultra-fast liquid chromatography-tandem mass spectrometry (UFLC-MS/MS): *in vivo* pharmacokinetics of apocarotenoids and carotenoids. *Molecules* 2021;26(6):1815.
[15] Wu S, Lu W, Cheng G, et al. DAPK1 may be a potential biomarker for arterial aneurysm in clinical treatment and activated inflammation levels in arterial aneurysm through NLRP3 inflammasome by Beclin1. *Hum Exp Toxicol* 2021;40(12_suppl):S563–S572.
[16] Xie L, Zhao Z, Chen Z, et al. Melatonin alleviates radiculopathy against apoptosis and NLRP3 inflammasomes *via* the Parkin-mediated mitophagy pathway. *Spine (Phila Pa 1976)* 2021;46(16):E859–E868.
[17] Shao S, Xu CB, Chen CJ, et al. Divanillyl sulfone suppresses NLRP3 inflammasome activation *via* inducing mitophagy to ameliorate chronic neuropathic pain in mice. *J Neuroinflammation* 2021;18(1):142.
[18] Huang Y, Cai T, Xia X, et al. Research advances in the intervention of inflammation and cancer by active ingredients of traditional Chinese medicine. *J Pharm Pharm Sci* 2016;19(1):114–126.
[19] Babuta M, Furi I, Bala S, et al. Dysregulated autophagy and lysosome function are linked to exosome production by Micro-RNA 155 in alcoholic liver disease. *Hepatology* 2019;70(6):2123–2141.
[20] Di Q, Zhao X, Tang H, et al. USP22 suppresses the NLRP3 inflammasome by degrading NLRP3 *via* ATG5-dependent autophagy. *Autophagy* 2023;19(3):873–885.